(4)

ANALYSIS OF SOME FRACTURE MECHANICS TEST PROCEDURES FOR DEFENCE RESEARCH APPLICATIONS

MRL-TR-89-11 AR-005-698

J. H. UNDERWOOD, I. A. BURCH AND M. Z. SHAH KHAN

ANALYSIS OF SOME FRACTURE MECHANICS TEST PROCEDURES FOR DEFENCE RESEARCH APPLICATIONS

J.H. Underwood*, I.A. Burch
and M.Z. Shah Khan

MRL Technical Report
MRL-TR-89-11

ABSTRACT

Analysis has been presented of six fracture mechanics specimens and associated test procedures. Stress intensity factor results, and displacement results in some cases, have been compared for each specimen with numerical results and limit solutions from the literature. The specimens and test procedures analyzed are a compact specimen for general fracture testing, a crack arrest compact specimen, a modified compact specimen for brittle coating tests, a bend specimen for stress-corrosion cracking tests, a round bar bend specimen, and a tensile panel for composite material tests. Comparison with literature results was used to draw conclusions regarding accuracy of stress intensity factor and displacement relations for the specimens.

* Exchange scientist at MRL from US Army Armament Research Development and Engineering Center, Watervliet, NY, USA.

Published by Materials Research Laboratory
Cordite Avenue, Maribyrnong, Victoria, 3032 Australia
Telephone: (03) 319 4499
Fax: (03) 318 4536

AR No. 005-698

Approved for Public Release

AUTHORS

Mr J.H. Underwood, currently a Senior Research Engineer at Benet Weapons Laboratory, received his Bachelor of Science degree in Mechanical Engineering from University of Massachusetts, USA in 1962. He received postgraduate instructions at New York University, USA, leading to the Master of Science degree in Metallurgy in 1965. In October 1965, he joined the Benet Weapons Laboratory and the direction of his research since then has been in basic and applied research in Fracture Mechanics, Engineering Mechanics and Mechanical Metallurgy. He has lectured and published scientific papers extensively. He is also a member of many research committees and was appointed as Chairman of ASTM Subcommittee E24.01 on Fracture Mechanics Tests Methods and 17th National Symposium on Fracture Mechanics. Mr Underwood was on an attachment to DSTO-MRL as a Visiting Scientist for a period of twelve months.

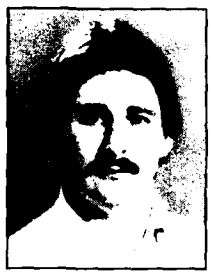

Mr I.A. Burch is an Experimental Officer in the fracture mechanics section of the Materials Division at MRL. He received a Diploma of Applied Science in Secondary Metallurgy from the Royal Melbourne Institute of Technology in 1983 and has been employed at MRL since 1982. He is mainly involved with the fracture and fatigue properties of Defence related materials.

Dr M.Z. Shah Khan, currently a Research Scientist at DSTO-MRL, received his Bachelor of Engineering degree in Mechanical Engineering from Osmania University, India, in 1978. He took postgraduate work at Iowa State University, USA, receiving the Master of Science degree in Metallurgy in 1981. In the beginning of 1983, he joined University of New South Wales, Australia, and obtained the Doctor of Philosophy degree in Metallurgy in 1986. In the middle of 1986 he assumed his present position where he has been active in the research of Metal Fatigue and Fracture particularly in support of the Naval Ship Structure research program.

CONTENTS

ANALYSIS OF SOME FRACTURE MECHANICS TEST PROCEDURES FOR DEFENCE RESEARCH APPLICATIONS

1. INTRODUCTION

In many areas of defence research work the fracture mechanics approach is used to characterize the growth of cracks. This always involves the use of fracture mechanics tests, in order to directly measure the crack growth resistance of materials and structural components. A number of refinements have been made in fracture mechanics test methods in the past two decades. Evidence of this can readily be seen in the current version of ASTM Standard E399 (1), Standard Test Method for Plane-Strain Fracture Toughness of Metallic Materials. This standard now includes seven annexes which describe a variety of specimen geometries and associated procedures for fracture mechanics tests. One important and useful relation which is supplied for each geometry is an accurate stress intensity factor, K, expression which applies over a wide range of relative crack depth, a/W. These expressions have been developed from results of numerical calculations of proven accuracy in combination with the appropriate deep crack limit solutions from the technical literature.

The purpose here is to compare some of these same numerical and limit solutions with the results and expressions from a number of fracture mechanics test and analysis procedures used at MRL. The test procedures chosen for comparison have been used for test geometries and materials which, for various reasons, preclude the use of standard test methods. Thus they have not always been subjected to rigorous and detailed logical analysis. Some of the procedures are in the process of becoming standard tests, by ASTM and other authorities. All of the test procedures are in the general category of elastic stress controlled fracture tests, as opposed to elastic-plastic or fully plastic tests.

2. METHODS

Results for each specimen and test procedure are discussed separately in the following sections, to avoid confusion with similar geometries and nomenclature. However the general method is similar in all cases. Comparison of the K expression for each specimen, and a displacement expression where appropriate, with results from the literature is used as a check on accuracy of the expressions over a range of a/W.

The important feature common to all the comparisons is the use of deep crack limit solutions for K and v, load-line-displacement. These limit solutions, for the geometry of the commonly used compact-type specimen, Fig. 1, are the following (2,3):

$$\lim_{a/W \to 1} (vEB/P)(1 - a/W)^2 = 15.80 \quad (1)$$

$$\lim_{a/W \to} (KBW^{1/2}/P)(1 = a/W)^{3/2} = 3.975 \quad (2)$$

where E is elastic modulus. Plots of normalized v and K results using the form of these limit solutions have the important property of remaining finite as well as relatively smooth and constant valued over a wide range of a/W, up to and including a/W = 1. This is a considerable help in comparing and analyzing results from different sources and in fitting expressions to v and K results. In contrast, other forms of results tend to infinity for deep cracks and consequently are of little use above about a/W = 0.8.

The advantage of the limit solutions is that, as $a/W \to 1$, the way in which v and $K \to \infty$ is counteracted by the way in which $(1 - a/W)^2$ and $(1 - a/W)^{3/2} \to 0$, in Eqs. 1 and 2, respectively. The result is a finite, nearly constant value of the product which, in addition, is an exact solution at a/W = 1. One other feature of Eqs. 1 and 2 worthy of note is their nondimensionality. This allows calculations in any consistent set of units with assurance that the effects of the critical physical parameters are included in the result.

For shallow cracks, $a/W \to 0$, the well known limit solution (2) is also of some use:

$$\lim_{a/W \to 0} \frac{K}{\sigma(\pi a)^{1/2}} = 1.122 \quad (3)$$

in which a is a shallow edge crack in a wide specimen subjected to a uniform tensile stress, σ. However, this shallow crack limit solution is sometimes overshadowed by the particular loading conditions of the specimen. Some types of loading result in a nonuniform tensile stress in the area of shallow cracks. For example, shallow cracks in compact-type specimens are dominated by the presence of the loading holes (see Fig. 1), and the shallow crack limit is of no use. For bend specimens the loading is remote enough from shallow cracks that Eq. 3 can be used. Forthcoming discussion of two types of bend specimen makes use of the shallow crack limit solution.

3. RESULTS AND DISCUSSION

3.1 MRL Compact Specimen

3.1.1 Background and Application

A fracture mechanics specimen similar to the ASTM compact specimen (1) is used at MRL for general purposes including measurement of plane-strain fracture toughness, K_{Ic}, J-integral fracture toughness, J_{Ic}, and fatigue crack growth rate. The specimen geometry was chosen to accommodate these three types of test and to match where possible the ASTM compact geometry, see Fig. 1. Finite element (4) and experimental compliance (5) analyses have been performed for the MRL compact to determine the effect of notch configuration on K and crack-mouth-displacement at the load-line, v. Considering the

different notch configurations shown in Fig. 1, some differences in K and v would be expected, particularly for small a/W. The objective of this section is to compare K and v results for the MRL and ASTM specimens and comment on the accuracy of the MRL results for use in fracture testing.

3.1.2 Comparison of Results

Figures 2 and 3 show the comparisons of v and K results, respectively, for the MRL and ASTM compact specimens. The v and K parameters used were chosen purposefully from the deep crack limit solutions, Eq. 1 and 2 as discussed previously.

The v results in Fig. 2 for the ASTM compact are based on Newman's collocation results of crack-mouth-displacement at the load-line (6). Saxena and Hudak (7) fitted an expression to these results:

$$vEB/P = \frac{(1 + a/W)^2}{1 - a/W} \quad 2.1630 + 12.219\ a/W - 20.065\ (a/W)^2 - 0.9925\ (a/W)^3 + 20.609\ (a/W)^4 - 9.9314\ (a/W)^5$$

for the range $0.2 < a/W < 0.975$ (4)

However, using the form of the limit solution, Eq. 1 a simpler expression was obtained here:

$$(vEB)/P\ (1 - a/W)^2 = 0.775 + 30.3\ a/W - 38.2\ (a/W)^2 + 22.3\ (a/W)^3 + 0.6\ (a/W)^4$$

for the range $0.2 < a/W < 1.0$ (5)

and is shown in Fig. 2. Equation 5 fits both the collocation and limit results within 1.0% for $0.2 < a/W < 1.0$.

The finite element and experimental compliance results for the MRL compact are seen in Fig. 2 to agree quite well. Both sets of results show a higher load-line displacement for the MRL geometry, which would be expected because the MRL notch configuration leaves less material to resist the load. The diminishing difference between the two specimens for large a/W, away from the location of configurational difference, is also expected. An expression was fitted to a combined set of v data, made up of finite element results from Ref. 2 for a/W of 0.36 to 0.76, results from Eq. 5 for a/W = 0.8 and 0.9, and the value of the deep crack limit (Eq. 1) for a/W = 1.0. The expression is:

$$(vEB)/P\ (1 - a/W)^2 = 2.13 + 36.9\ a/W - 62.5\ (a/W)^2 + 44.7\ (a/W)^3 - 5.4\ (a/W)^4$$

for the range $0.36 < a/W < 1.0$ (6)

which fits the finite element results to within 0.6% and the collocation and limit results within 1.2%.

The K results in Fig. 3 for the ASTM compact are Newman's earlier collocation data (8) and the expression fit to the data, the K expression used in ASTM Method E399 (1):

$$(KBW^{1/2}/P)\ (1 - a/W)^{3/2}/(2 + a/W) = 0.886 + 4.64\ a/W - 13.32\ (a/W)^2 + 14.72\ (a/W)^3 - 5.6\ (a/W)^4$$

for the range $0.2 < a/W < 1$ (7)

Also shown in Fig. 3 are K data for a compact specimen of the ASTM geometry but without holes; a distributed load applied on the crack faces replaces that on the hole surfaces (8). The difference between these no-hole K results and those of the standard ASTM compact specimen gives some indication of the difference which would be expected between the MRL and ASTM compact specimens. Note that the no-hole and ASTM compact K values agree within about 1% for $a/W > 0.4$. However, it is clear that the finite element and experimental compliance K results for the MRL specimen rise above those for the ASTM specimen. Of most concern are the consistently high finite element values for $a/W > 0.6$. For these geometries, with the crack well beyond the area of configurational difference at the notch, the MRL and ASTM results should agree closely, as the deep crack limit is approached. Although this area of disagreement is outside the K_{Ic} test range, it is an area commonly used in fatigue crack growth rate tests.

3.1.3 Conclusions

The v results from finite element analysis (4), combined with deep crack results from the ASTM compact expression and the limit solution, give the v expression for the MRL compact specimen, Eq. 6 above. It is believed to be accurate within 2% over the range $0.36 < a/W < 1$. Experimental compliance results (5) are in general agreement with Eq. 6 and provide a direct physical check.

The K expression for the standard ASTM compact specimen, Eq. 7 above, should also apply to the MRL compact specimen with an accuracy within 2% over the range $0.4 < a/W < 1$. Finite element and experimental compliance results are in general agreement with Eq. 7 for intermediate crack length, a/W from 0.4 to 0.6. For deeper cracks, collocation and limit solution results of established accuracy agree well with Eq. 7.

3.2 Crack Arrest Compact Specimen

3.2.1 Background and Application

A compact-type specimen is at present being developed for use in wedge-loaded crack arrest fracture toughness tests (9,10). The important compliance expression for this type of test and specimen is the ratio of stress intensity factor to crack-mouth-displacement, K/δ, as a function of relative crack length, a/W (see Fig. 4). This expression is used for calculating crack arrest fracture toughness (9,10) and is suitable for other tests using wedge loading, such as some stress-corrosion cracking tests. The objective in this section is to compare two sets of K/δ results, one based on experimental compliance (9) and the other based on collocation calculations (6,8). Each set of results also is compared with the appropriate deep crack limit solution, and discussion is offered regarding the accuracy of the two sets of results.

3.2.2 Comparison of Results

The basis of the comparison is the following dimensionless parameter, Y:

$$Y = \frac{KW^{1/2}/\delta E}{(1 - a/W)^{1/2}} \tag{8}$$

This parameter was used because it is the form of the deep crack limit solution (2) for this specimen type*:

$$\lim_{a/W \to 1} \frac{KW^{1/2}/\delta E}{(1 - a/W)^{1/2}} = 0.2013 \tag{9}$$

Note that Eq. 9 can be obtained by combination of Eqs. 1 and 2 and the relation $\delta = 5v/4$ for $a/W \to 1$. The form of Eq. 9 has the important property of remaining within the range 0.20 to 0.35 over the a/W range of interest. Comparison is not impaired by values tending toward 0 or ∞, hence maximum resolution is possible.

The comparison of Y versus a/W results from experiment and collocation is shown in Fig. 5 and Table 1. Equation 10, obtained from the experimental compliance results of reference 9 and specified as the K/δ relation for reference 10, is:

$$Y = \frac{2.24\ (1.72 - 0.9\ a/W + (a/W)^2)}{9.85 - 0.17\ a/W + 11\ (a/W)^2} \tag{10}$$

for the range $0.35 < a/W < 0.85$. Equation 11, fitted to the collocation results of references 6 and 8, is (11):

$$Y = 0.748 - 2.176\ a/W + 3.56\ (a/W)^2 - 2.55\ (a/W)^3 + 0.62\ (a/W)^4 \tag{11}$$

for the range $0.2 < a/W < 1$. The deep crack limit solution ($a/W = 1$) is also shown in Fig. 5 and Table 1.

The comparison shows that the two sets of results agree well for a/W between 0.4 and 0.6 and diverge for lower and higher a/W. The difference for low a/W may be caused by differentiation of compliance data near the end point of the data, an inherent limitation of the experimental compliance method. This difference between the results at low a/W is of little concern, in the present argument, lying below the range of a/W used to calculate crack arrest fracture toughness and seldom used in other tests. For high a/W the maximum difference between the two results is more than 6% at an a/W of about 0.8. Unlike some other fracture tests, this high value of a/W is important for the crack arrest test, because many of the final, most critical measurements are made on crack arrests occurring at an a/W of about 0.8.

---

* A plane-stress crack-mouth-displacement analysis is considered to be correct here because most of the specimen is allowed to deform in the thickness direction. Only a small portion of the specimen near the crack tip is subjected to plane-strain condition and the associated constraint in the thickness direction. This small portion has little effect on the global crack-mouth-displacement.

One possible cause of the disagreement at high a/W is the two-dimensional nature of the collocation analysis as opposed to the three dimensional experiments (9) which involved the use of side grooves. However, any effects of this general difference between experiment and analysis would be expected over the whole range of a/W, not just at high a/W. Another possible cause which can be eliminated on this same basis is the use of collocation displacements with an inappropriate choice of boundary conditions. Regardless of the choice, plane-stress or plane-strain, discrepancies only at high a/W would not be expected. In the work here, Newman's plane-stress displacements (6) were used to obtain Eq. 11 because crack-mouth-displacement is a global parameter (see Footnote on page 11). If plane-strain displacements had been used the difference between experiment and analysis would have been about 15% rather than 6%.

Two aspects of compliance experiments which can result in errors, particularly for large a/W, are notch width and plastic zone effects. Both the width of the notch and the plastic zone at the notch tip can become significant in size relative to the remaining ligament, (W-a), which is the controlling dimension at large a/W. Furthermore, both of these effects would be expected to increase the effective notch length, thus increasing δ and decreasing Y. This could explain the disargreement between experiment and analysis. The experiment, even though it is a direct model of the physical problem, is unfortunately subject to notch and plastic zone effects which limit the accuracy of the model and mask the fundamental benefits of the approach.

3.2.3 Conclusions

The K/δ expression based on collocation results, Eq. 11, is more accurate than the experimental compliance expression, particularly for large a/W. Equation 11 is believed to be accurate to within 1% over the range $0.2 < a/W < 1$. The collocation results agree well with experiment for intermediate a/W, where experimental compliance methods can be used as a direct check on analysis. At large a/W the collocation results converge closely upon the deep crack limit solution, whereas the experimental results are affected by inherent experimental difficulties.

3.3 Modified Compact Specimen for Brittle Coating Tests

3.3.1 Background and Application

A compact type specimen has been used by Ostojic (12) for measuring the fracture toughness of oxide coatings. The tests and related analysis are made difficult by the small thickness of coating. A nominal 0.4 mm thick oxide layer was thermally sprayed onto one half of the steel specimen which was then epoxy bonded to the second half, to make up the composite specimen shown in Fig. 6. By careful experimental control, failure can be made to occur at the approximate mid-plane of the oxide layer, as shown in Fig. 6. Nevertheless, for deep cracks, $a/W > 0.6$, a significant and unexplained decrease in apparent fracture toughness was noted for all materials tested. Ostojic suggests that K_{Ic} tests may need to be restricted to crack depths less than $a/W = 0.6$, because of a different type of bending behaviour for deeper cracks. The objective here is to analyse the test procedure and results in an effort to explain this apparent dependence of K_{Ic} on crack depth. With attention to K expressions from the literature, it may be possible to obtain more reliable K_{Ic} results.

3.3.2 Comparison of Results

Figure 7 shows the variation with crack depth of both applied stress intensity factor, K, and the measured fracture toughness, K_{Ic}, for one of the oxides tested (12). The K_{Ic} data are for stable crack growth from one specimen of aluminium oxide (Al_2O_3) which was observed to undergo cohesive failure within the oxide layer. Note that for $a/W > 0.6$ the K_{Ic} decreases significantly, by about 40% at $a/W = 0.8$.

The two curves in Fig. 7 are expressions for applied K for the compact specimens, using the K parameter described earlier (Section 3.1.2). The expression for the ASTM compact specimen is that given earlier as Eq. 7, for the standard height-to-width ratio, $H/W = 0.60$. The K expression for the modified compact specimen, with $H/W = 0.56$, is:

$$Y_{mod} = (K_{mod} BW^{1/2}/P) (1 - a/W)^{3/2}/(2 + a/W) \qquad (12)$$

and K_{mod} is obtained from experimental compliance results (12) as:

$$K_{mod} = P \frac{(E f^{1/2})}{1 - \nu^2} \qquad (13)$$

where Poisson's ratio $\nu = 0.19$, elastic modulus $E = 23$ GPa (13), and f is a compliance parameter, a function of a/W with units of $(Nm)^{-1}$. It should be noted that the scales for Fig. 7 were selected for an easy comparison of the crack-length dependence of applied K (Eq. 12) and the K_{Ic} data. The only significance to the similar placement on the plot of K and K_{Ic} values is that it allows a comparison of a/W dependence of the two sets of values.

3.3.3 Conclusions

Consideration of the two K expressions and the K_{Ic} data in Fig. 7 suggests the source of the apparent crack length dependence of K_{Ic}. For $a/W > 0.6$ the modified compact K expression is incorrect. The K expression for any compact type specimen, regardless of H/W ratio, should approach the deep crack limit solution, Eq. 2. It is clear that Eq. 12 diverges from the limit for $a/W > 0.6$, so it is incorrect in this range. Taking this into consideration, it appears that there is no dependence of K_{Ic} on crack length for the materials tested.

The results of Fig. 7 also can be used to comment on the accuracy of Eq. 12 for $a/W < 0.6$, although with less certainty than the above conclusion. The modified compact K expression is more than 50% lower than the ASTM expression for $a/W < 0.6$, whereas the most significant difference in overall geometry, $H/W = 0.56$ compared with 0.60, would suggest that the modified K should be, on average, about 3% higher (14). This significant difference between the expressions may be due to the uncertainty in the value of E in Eq. 13. The specimen is a composite of steel, epoxy and oxide, and E for the oxide as tested may be different from that given in Reference 13. These factors could explain the lower applied K for the modified compact specimen for intermediate crack lengths.

3.4 Bend Specimen for Stress-Corrosion Cracking Tests

3.4.1 Background and Application

Current work at MRL (15) uses cantilever-loaded bend specimens to characterize the stress-corrosion cracking behaviour of sintered tungsten alloys. The environment and loading conditions are an immersion in 3.5% NaCl aqueous solution followed by sustained loading in 95% relative humidity air. The detailed test procedures and results are the subject of a forthcoming report (15). The methods for calculating the critical fracture mechanics parameters will be examined here and compared with methods from the literature.

The specific application for the stress-corrosion cracking tests is sintered tungsten rods used as kinetic energy penetrators for launch from rifles or cannons. Such penetrators can be subjected to aqueous NaCl environment in storage (15). If sustained tensile stress is also present, due to a fabrication process for example, stress-corrosion cracking could occur. Cantilever loading is often used for stress-corrosion cracking investigations, so the analysis here may have other applications.

3.4.2 Comparison of Results

Figure 8 shows the type of geometry and nomenclature. Analysis of this type of fracture test will be given in six areas, K, Δ, and a/W expressions, specimen length and notch width effects, and compliance unloading procedures for measuring a/W.

(a) The K for a long cantilever-bend specimen is closely approximated by that for a pure bend specimen (14):

$$KBW^{3/2}/M = 6\ (2\ \tan \tfrac{\pi}{2}\tfrac{a}{W})^{1/2}\ \frac{(0.923 + 0.199\ (1 - \sin \tfrac{\pi}{2}\tfrac{a}{W})^4)}{\cos \tfrac{\pi}{2}\tfrac{a}{W}} \qquad (14)$$

for the range $0 < a/W < 1$ where the bending moment, $M = PL$. A measure of how long the cantilever bend specimen must be for a close approximation is discussed in item (d), below. For cantilever or pure bending it is easy to show that Eq. 14 properly approaches the shallow crack limit (2):

$$\lim_{a/W \to 0} KBW^{3/2}/M = 6\ (1.122\ (\pi\ a/W)^{1/2}) \qquad (15)$$

Using the identity $\tan x = 1/\tan(\pi/2 - x)$ and other trigonometric relationships, it can be shown that Eq. 14 approaches the deep crack limit (2):

$$\lim_{a/W \to 1} KBW^{3/2}/M = \frac{3.975}{(1 - a/W)^{3/2}} \qquad (16)$$

(b) The Δ expression for a long cantilever-bend specimen, following a similar argument to (a), is (14):

$$\Delta EBW/M = 24(a/W)\ [0.8 - 1.7\ a/W + 2.4\ (a/W)^2 + \frac{0.66}{(1 - a/W)^2}] \qquad (17)$$

for the range $0 < a/W < 1$ and the deep crack limit solution, properly approached, is (3):

$$\lim_{a/W \to 1} \Delta EBW/M = \frac{15.80}{(1 - a/W)^2}. \qquad (18)$$

(c) The crack length expression used here is essentially that of Joyce et al. (16), but in simpler form:

$$a/W = 1 - 3.83C - 1.81C^2 + 32.3C^3 - 44.2C^4 - 52.7C^5$$

$$C = \frac{1}{(\Delta EBW/M)^{1/2} + 1} \qquad (19)$$

for the range $0.3 < a/W < 1$. Note that Eq. 19 has a more limited range of applicability than Eq. 17. As with Eqs. 14 and 17, Eq. 19 is a close approximation for relatively long cantilever beams. The beam length effect on K, Δ, and a/W calculations is discussed next.

(d) It is suggested that the ratio of beam deflection due to pure bending, y_{bend}, to that due to shear, y_{shear}, gives a measure of how closely a cantilever beam approximates a pure bending beam. If the length of the cantilever beam is large then y_{bend}/y_{shear} is large, and the cantilever beam behaves similarly to the pure bend beam. Expressions for y_{bend} and y_{shear} are available from Roark and Young (17):

$$EBy_{bend}/P = 6\ L\ell^2/W^3 \qquad (20)$$

$$EBy_{shear}/P = 2.4\ (1 + \nu)\ \ell/W \qquad (21)$$

Equations 20 and 21 can be used to calculate y_{bend}/y_{shear} for a particular beam. As an example, for the geometry shown in Fig. 8, $\ell/W = 1$, $L/W = 5$, and for $\nu = 0.3$, $y_{bend}/y_{shear} = 9.6$. Since y_{bend} is about ten times y_{shear}, pure bending is predominant for this example, and Eqs. 14, 17 and 19 are reasonable approximations. For y_{bend}/y_{shear} smaller than this, caution is advised, particularly for displacement and inverse displacement calculations, Eqs. 17 and 19.

(e) Another check on specimen geometry which may be of interest is the notch width effect. For this concern the assumption is made that the ratio of crack-mouth-displacement, Δ, to an outer fibre uniform strain displacement, (assuming no notch or crack) Δ_ϵ, gives an indication of an excessively wide notch. If Δ/Δ_ϵ is large, Δ is controlled by the notch depth, a/W (as in Eq. 17), and there is little additional effect on Δ due to an excessive notch width. An expression for Δ_ϵ can

be obtained from the relation for outer fibre strain in bending, using a gauge length, n:

$$\Delta_\epsilon \, EBW/M = 6 \, n/W \qquad (22)$$

For geometry n/W = 0.1 and a/W = 0.5, the ratio Δ/Δ_ϵ from Eqs. 17 and 22 is 63.8. For this geometry it is clear that effects on Δ due to notch width are negligible.

(f) Analysis of the stress-corrosion cracking data (15) includes the use of a compliance method for measuring crack length. It is worthy of discussion because it can significantly improve the accuracy and consistency of the results. In addition, it is a method which is commonly applied to J_{Ic} and fatigue crack growth rate data, so its use in this work may be of interest.

The key features of the compliance method as applied to the stress-corrosion cracking data can be described in relation to Table 2, representative data from the work of Shah Khan et al. (15). The sustained loading in this data corresponded to an initial K of 46 MPa $m^{1/2}$, followed by a 34% unloading for compliance measurement. The calculated a/W from the first unloading, 0.519, was in good but not exact agreement with the value measured from the fracture surface after the test, 0.509. To improve the accuracy of a/W calculated from subsequent unloadings, an effective modulus, E^* was used, which differed from the typical modulus (370 GPa) by the ratio 0.509/0.519:

$$E^* = E \, \frac{(\Delta EBW/M)_{measured}}{(\Delta EBW/M)_{calculated}} \qquad (23)$$

As would be expected, the use of E^* produced very close agreement between measured a/W and that calculated from unloading compliance. Thus the subsequent calculated a/W values, which describe the stress-corrosion crack growth, have improved accuracy. As is often the case in this type of test, it was not possible to directly compare measured and calculated a/W at the end of the test. The crack growth was rapid at the end, and the last programmed unloading did not occur at the same time as final failure, so a comparison of the a/W value from unloading with that from the fracture surface just before final failure could not be made.

It should be noted that the earlier fracture surface measurement from which the effective modulus was determined was a five-point measurement. The mean of the two a/W values form the specimen surfaces and the three interior quarter-point values was used. Although this five-point a/W would be inappropriate for defining a K_{Ic} failure point, which is specimen-interior dominated, it is considered to be a suitable value for comparison with a compliance measurement of a/W. The surface values of crack length are certainly included in a compliance measurement of a/W. Furthermore, for the common case of a tunnelled crack, the smaller surface values of a/W dominate the compliance. So the surface values should be included in a measurement of a/W which is compared with a compliance measurement.

3.4.3 Conclusions

Equations 14, 17 and 19 are close approximations of K, Δ and a/W for a cantilever beam providing the beam is long enough. A comparison of the beam deflection due to pure bending with that due to shear, Eqs. 20 and 21, provides a measure of adequate beam length. For a long cantilever beam, Eqs. 14, 17 and 19 are believed to be accurate within 1%, 2% and 2% respectively, for the stated ranges of a/W.

A compliance-unloading measure of a/W combined with the use of effective modulus, Eq. 23, results in improved accuracy of stress-corrosion crack growth data for the cantilever beam specimen. The effective modulus is properly calculated using a five-point measure of a/W from the fracture surface, to take account of the important surface crack lengths which are naturally included in the measurement of a/W from the unloading compliance.

3.5 Round Bar Bend Specimen

3.5.1 Background and Application

Bush (18) apparently was the first to perform comprehensive analysis of the round bar bend specimen for fracture testing applications. His application was power generation turbine rotors. Woodward (19) has suggested the use of this geometry for fracture testing of sintered tungsten rod stock used for kinetic energy projectiles, a useful suggestion considering the difficulty to machining sintered tungsten. A round bar with a notch added can be used for fracture tests with little or no additional machining. Bush's work will be used here along with limit solutions to propose a test specimen geometry and associated K expression for use in fracture testing. A wide range of crack depth relative to bar diameter, a/D, will be considered, to accommodate different types of fracture tests.

3.5.2 Comparison of Results

Figure 9 shows the basic elements of a round bar bend specimen for fracture testing and some associated nomenclature. It is is the same basic geometry as that of Bush (18), who obtained experimental compliance K results for a bar with S/D = 3.33 and one with S/D = 6.67. His results are shown in Fig. 10 along with limit solutions and two expressions based on both experimental and limit solution results.

The deep crack limit for a round bar is different from that for a rectangular bar. Combining the rectangular bar limit expression (Eq. 16) with W = D:

$$\lim_{a/D \to 1} \quad (KBD^{3/2}/M)\,(1 - a/D)^{3/2} = 3.975 \tag{24}$$

with an expression for the chordal length of a circular segment, to account for the changing B dimension as a/D → 1:

$$B = 2D\,(a/D)^{1/2}\,(1 - a/D)^{1/2} \tag{25}$$

gives the deep crack limit for the round bar:

$$\lim_{a/D \to 1} \quad (KD^{5/2}/M)\,(1 - a/D)^{2} = 1.988 \tag{26}$$

The shallow crack limit for a round bar is also affected by changing crack dimensions as a/D → 0. The usual limit solution (2) is written in terms of a', an effective crack depth which accounts for the variations in depth of a shallow crack in the shape of a circular segment, see Fig. 11:

$$\lim_{a/D \to 0} \quad (K/\sigma D^{1/2}) \;/\; (a'/D)^{1/2} = 1.122 \tag{27}$$

where $\sigma = 32M/\pi D^3$, the relationship for the outer fibre stress, σ, for a round bar (20). The ratio a'/a is determined from the moments of inertia of a circular segment, I_s, and a rectangle, I_r, with the same overall dimensions a and B:

$$a' = a\ (I_s/I_r) \tag{28}$$

Expressions for I_s and I_r are available (20):

$$I_r = Ba^3/12 \tag{29}$$

and

$$\lim_{a/D \to 0} I_s = 0.01143\ D^4\alpha^7/16 \tag{30}$$

where for $a/D \to 0$, $\alpha = B/D$, and B/D can be written in terms of a/D using Eq. 25. Combining Eqs. 25, 27-30 gives the shallow crack limit for a round bar:

$$\lim_{a/D \to 0} (KD^{5/2}/M)\ (a/D)^{1/2} = 15.00 \tag{31}$$

The form of both the deep and shallow crack limits, Eqs. 26 and 31, was used to obtain a K parameter which converges to both limits:

$$Y_{rb} = (KD^{5/2}/M)\ (1 - a/D)^2/(a/D)^{1/2} \tag{32}$$

This was the parameter used for plotting the experimental compliance results and the K expressions in Fig. 10. One K expression was fitted to a combined set of data made up of the ten experimental compliance data for S/D = 6.67 and $0.15 < a/D < 0.70$ and the two limit solutions, $Y_{rb} = 1.988$ and 15.00. The experimental data for $a/D < 0.15$ were excluded from the fit to allow the expression to converge to the shallow crack limit, believed to be more accurate than the shallow crack experimental data. The expression, using M = PS/4, is:

$$(KD^{5/2}/PS)\ (1 - a/D)^2/(a/D)^{1/2} = 3.75 - 10.05\ a/D + 17.93\ (a/D)^2 - 19.07\ (a/D)^3 + 7.94\ (a/D)^4 \tag{33}$$

for the range $0 < a/D < 1$ and S/D = 6.67. Equation 33 fits the experimental results within 2.2% and the two limits within 0.6%. A second K expression was fitted to five S/D = 6.67 experimental data which were adjusted slightly to correspond to S/D = 4.0, a more commonly used bend specimen geometry (1). The data for $0.4 < a/D < 0.6$ were decreased by 2%, a factor obtained from Tada et al. (14) for rectangular bend specimen K results over a range of S/D. This expression, also fitted to the shallow and deep crack limits (Eqs. 26 and 31) is:

$$(KD^{5/2}/PS)\ (1 - a/D)^2/(a/D)^{1/2} = 3.75 - 10.38\ a/D + 17.85\ (a/D)^2 - 16.78\ (a/D)^3 + 6.06\ (a/D)^4 \tag{34}$$

for the range $0 < a/D < 1$ and $S/D = 4.0$. Equation 34 fits the adjusted experimental results within 1.1% and the two limits within 0.6%. Note that Eq. 34 is about 2% below Eq. 33 for $a/D = 0.4$, as expected, but for deeper cracks it rises above Eq. 33. This indicates that the experimental compliance result for $a/D = 0.7$ may be inaccurate, and its exclusion from the input data may have improved the accuracy of Eq. 34.

One additional point which should be discussed is the flat surfaces shown in Fig. 9 at the locations of contact between specimen and support pins. These surfaces add to the complexity of the specimen, but in general they are required to ensure a known value of applied K for the round bar specimen. With no flat surfaces, the contact between specimen and pin would start as a point contact which could lead to a significant plastic identation in the specimen and loss of the required free rolling loading condition. The small amount of material removed to make the flat surfaces and their remoteness from the crack result in no significant effect on K.

3.5.3 Conclusions

The round bar bend specimen and associated K expression in Fig. 9 and Eq. 34, respectively, can be used for general fracture mechanics testing, including K_{Ic} and fatigue crack growth rate tests. The K expression is believed to be accurate within 2% for all crack lengths.

3.6 Tensile Panel for Composite Material Tests

3.6.1 Background and Application

Fracture toughness tests of carbon/polymer sheet are underway at MRL (21). One purpose of the tests is to determine fibre orientation and notch geometry conditions for which continuum fracture mechanics can be used to characterize the fracture behaviour of carbon/polymer sheet. Details of the tests and results will be given in a forthcoming report (21). The purpose here is to describe stress intensity factor, displacement and crack length expressions for use in the fracture tests with center-cracked tensile panels. A tensile panel is well suited to carbon/polymer materials, because they are commonly made as sheet and usually subjected to primarily tensile stress. Compressive stress, even in only part of a specimen (due to bending), can lead to full thickness or local fibre compressive buckling failure.

The expressions for K, crack-mouth-displacement at crack mid-length, u, and a/W in terms of u are obtained from the literature, modified where appropriate, and compared with other results of known accuracy. The expressions, although based on continuum mechanics, can be useful for composite materials. For some cases, the deformation and fracture behaviour of composite materials may be so similar to that for a continuum that the continuum approach is totally adequate and any other approach is unduly complex. For other cases, the continuum approach may prove futile. Accurate and complete fracture test and analysis procedures will help in separating one case from another.

3.6.2 Comparison of Results

The tensile panel geometry and nomenclature is shown in Fig. 12, along with some details of a typical test arrangement. For composite materials the load nearly always is applied to sheet specimens via fixtures which attach to the specimen ends, in the general manner shown in Fig. 12. Such loading produces lines of approximately uniform displacement at a distance h from the crack line, so this is the loading condition which should be modelled in

K and u expressions.

A commonly used expression for K for a centre-cracked panel is Feddersen's (22):

$$KBW^{1/2}/P = (\pi\ a/W \sec\ (\pi\ a/W)^{1/2} \qquad (35)$$

for the range $0 < 2a/W < 0.9$ and $h/W > 0.75$. A check on how closely this expression models uniform displacement loading conditions was recently made by Newman and Tan (23). They used a boundary-force method to calculate K values for a centre-cracked sheet with $h/W = 0.75$. The values compare well with those from Eq. 35, as shown in Table 3. A useful modification to Eq. 35 is that which accounts for an eccentricity, e, of the crack centerline relative to the panel centerline (24):

$$KBW^{1/2}/P = (\pi\ a/W \sec\ (\frac{\pi\ a/W}{1 - 2e/W}))^{1/2} \qquad (36)$$

for the range $0 < 2a/W < 0.9$ with $h/W > 0.75$ and $e/W < 0.15$. Equation 36 can be used to handle cases in which the centre crack is made off-centre or grows off-centre.

The K expression for a centre-cracked panel, Eq. 36, applies over a wide range of test geometries, including relatively short specimens and those with some crack eccentricity, so it is quite useful. It converges to the shallow crack limit (14) (for $e = 0$):

$$\lim_{2a/W \to 0} (KBW^{1/2}/P) \ / \ (\pi\ a/W)^{1/2} = 1.00 \qquad (37)$$

Although it does not converge to the deep crack limit (14), it is a reasonable approximation for quite deep cracks, $2a/W = 0.9$.

An expression for u, similar in form to that of Tada et al. (14), is the following, for uniform displacement loading conditions and plane-stress boundary conditions:

$$BEu/P = -0.14(2a/W) - 1.04(2a/W)^2 + 0.21(2a/W)^3 - 2.14 \ln (1 - 2a/W) \qquad (38)$$

for the range $0.1 < 2a/W < 0.8$ and $h/W > 0.75$. Equation 38 was fitted here within 0.5% to Newman's results (6) for the range $0.1 < 2a/W < 0.8$ and $h/W = 2.0$ and the same loading and boundary conditions. The logarithmic term in the expression is the deep crack limit (14) which dominates as $a/W \to 1$, so the expression has the correct form for deep cracks. Table 3 shows that for quite short specimens, with $h/W = 0.75$, Eq. 38 agrees with the recent numerical results (23) within about 2%.

An expression for $2a/W$ in terms of u, fitted here to Newman's results (6) to within an absolute error in $2a/W$ of 0.007, is:

$$2a/W = 1.23 + 2.07\ X - 12.33\ X^2 + 10.08\ X^3 \qquad (39)$$

$$X = \frac{1}{(BEu/P)^{1/2} + 1}$$

for the range $0.1 < 2a/W < 0.8$ and $h/W > 0.75$. The form used is that of Saxena and Hudak (7), often used for a/W expressions.

3.6.3 Conclusions

The K, u and 2a/W expressions of Eqs. 36, 38 and 39, respectively, can be used for centre-cracked panel testing and analysis, with an estimated accuracy of within 2%. The same expressions with some tighter geometric limits, that is with $e/W < 0.05$ and $h/W > 1.5$, have better accuracy, estimated to be within 1%.

4. OVERVIEW AND CONCLUSION

The common objective in each of the six examples was to apply shallow and deep crack limit solutions in determining accurate K and displacement expressions. Usually, existing solutions were acceptably accurate for mid-crack lengths but for various reasons inadequate at extremes. The best example of this was the determination of a K expression for the round bar bend specimen, Section 3.5. Once the shallow and deep crack limit solutions were obtained, their combination with a few mid-crack-length experimental compliance results produced an accurate expression for all crack lengths. Other examples here clearly showed the importance of limit solutions by the poor results obtained when the limits were not used.

Both experimentalists and numerical analysts alike can derive considerable benefit from an examination of the available solutions to a given fracture mechanics problem and, in particular, the closed form limit solutions. The high degree of precision of many closed form solutions can greatly enhance the value of their efforts.

5. ACKNOWLEDGEMENTS

We are pleased to acknowledge J.C. Ritter for helpful comments during all stages of the work, M.T. Butler and K.A. O'Connell for preparing the manuscript, and L.R.F. Rose of Aeronautical Research Laboratories for a thorough and useful review.

6. REFERENCES

1. Standard test method for plane-strain fracture toughness of metallic materials (1986). Annual Book of ASTM Standards, Vol 03.01, (ASTM, Philadelphia), pp. 522-557.

2. Benthem, J.P. and Koiter, W.T. (1973). Asymptotic approximations to crack problems. In G.C. Sih (ed) Mechanics of Fracture, 1, pp. 131-178 (Noordhoff, Leyden, The Netherlands).

3. Tada, H., Paris, P.C. and Irwin, G.R. (1973). The stress analysis of cracks handbook, (Del Research Corporation, Hellertown, PA), Section 9.

4. Heller, M. and Paul, J. (1985). Numerical compliance and stress intensity factor calibrations of MRL compact specimens (Report ARL-STRUC-TM-421). Melbourne, Vic.: Aeronautical Research Laboratories.

5. Clark, G. (Materials Research Laboratories) (1985) Unpublished results.

6. Newman, J.C. Jr. (1976). Crack-opening displacements in center-crack compact and crack-line wedge-loaded specimens (Report NASA TN D-8268). Hampton, VA: NASA Langley Research Center.

7. Saxena, A. and Hudak, S.J. Jr. (1978). Review and extension of compliance information for common crack growth specimens. International Journal of Fracture, **14**, 453-468.

8. Newman, J.R. Jr. (1974). Stress analysis of the compact specimen including the effects of pin loading. In, Fracure Analysis, ASTM STP 560, pp 105-121 (ASTM, Philadelphia).

9. Crosley, P.B. and Ripling, E.J. (1981). Development of a standard test for measuring K_{Ia} with a modified compact specimen (Report ORNL/Sub-81/7755/1). Oak Ridge, TN: Oak Ridge National Laboratory.

10. Proposed ASTM standard test method for determining the plane-strain crack-arrest fracture toughness, K_{Ia}, of ferritic steels, ASTM Committee E 24 Ballot, American Society for Testing and Materials, Philadelphia, Dec 1986.

11. Underwood, J.H. and Newman, J.C. Jr. (1987). Comparison of compliance results for the wedge-loaded compact specimen. Submitted to Journal of Testing and Evaluation.

12. Ostojic, P. (1986). The adhesion of thermally sprayed coatings, Doctoral Thesis, Monash University, Dept. of Materials Engineering, Clayton, Vic.

13. Glandus, J.C., Platon, F. and Boch, P. (1979). Measurement of the elastic moduli of ceramics. International Journal of Materials in Engineering Applications **1**, 243-246.

14. Tada, H., Paris, P.C. and Irwin, G.R. (1973). The stress analysis of cracks handbook, (Del Research Corporation, Hellertown, PA), Section 2.

15. Shah Khan, M.Z., Underwood, J.H. and Burch, I.A. Stress-corrosion cracking of liquid-phase sintered tungsten alloys, Materials Research Laboratory (to be published).

16. Joyce, J.A., Hasson, D.F. and Crowe, C.R. (1980). Computer data acquisition monitoring of the stress corrosion cracking of depleted uranium cantilever beam specimens. Journal of Testing and Evaluation **8**, 293-300.

17. Roark, R.J. and Young, W.C. (1975). Formulas for stress and strain. New York: McGraw-Hill Book Co., pp. 101-185.

18. Bush, A.J. (1976). Experimentally determined stress intensity factors for single-edge-crack round bars loaded in bending. Experimental Mechanics **16**, 249-257.

19. Woodward, R.L. (Materials Research Laboratories) (1987). Personal communication.

20. Roark, R.J. and Young, W.C. (1975). Formulas for stress and strain. New York: McGraw-Hill Book Co., pp. 61-69.

21. Underwood, J.H. and Burch, I.A. Effects of notch geometry and moisture on fracture strength of carbon/polymer sheet, Materials Research Laboratory (to be published).

22. Feddersen, C.E. (1966). Discussion in Current status of plane strain crack toughness testing of high strength metallic materials, ASTM STP 410, pp. 77-79 (ASTM, Philadelphia).

23. Newman, J.C. and Tan, P. (1986). Response to ballot on ASTM method E647, Nov 18, 1986 (ASTM, Philadelphia).

24. Tada, H., Paris, P.C. and Irwin, G.R. (1973). The stress analysis of cracks handbook, (Del Research Corporation, Hellertown, PA), Section 11.

Table 1 Comparison of K/δ results for Wedge-loaded Compact Specimen

a/W	$\frac{KW^{1/2}/\delta E}{(1 - aW)^{1/2}}$				
	Collocation Data; Ref.(6,8)	Experimental Compliance Eq. 10	Difference from Collocation Data %	Collocation; Eq. 11	Difference from Collocation Data %
0.2	0.4360	-	-	0.4358	0.0
0.3	0.3526	-	-	0.3518	-0.2
0.4	0.3001	0.2950	-1.7	0.2999	-0.1
0.5	0.2703	0.2721	+0.7	0.2700	-0.1
0.6	0.2543	0.2516	-1.1	0.2536	-0.3
0.7	0.2443	0.2341	-4.2	0.2434	-0.4
0.8	0.2339	0.2193	-6.2	0.2340	0.0
	Limit Eq. 9:				
1.0	0.2013	0.1971	-2.1	0.2020	+0.3

Table 2 Calculated and measured crack length from sintered tungsten specimen dipped in 3.5% NaCl aqueous solution followed by sustained loading in 95% relative humidity air (15); E = 370 GPa; effective modulus, $E^* = 349.5$ GPa (Eq. 23)

Sustained Load Time Increment	$\Delta EBW/M$ Unloading	a/W Calculated Eq. 19	a/W Measured 5 point	$\Delta E^*BW/M$ Unloading	a^*/W Calculated Eq. 19
0	42.7	0.519	0.509	40.3	0.509
1	43.8	0.524	-	41.4	0.514
2	46.8	0.536	-	44.2	0.526
3	51.3	0.552	-	48.5	0.542
4	53.7	0.559	-	50.7	0.550
5	64.4	0.590	-	60.9	0.581
6	-	-	0.664	-	-

Table 3 Stress intensity factor, K and mid-length crack line displacement, u for center-cracked tensile panels

2a/W	$KBW^{1/2}/P\ (\pi a/W)^{1/2}$ Uniform Displacement		BEu/P Uniform Displacement; Plane Stress		
	Newman(23) h/W = 0.75	Eq.35	Newman(23) h/W = 0.75	Newman(6) h/W = 2.0	Eq. 38
0.2	1.043	1.025	0.418	0.410	0.410
0.5	1.196	1.189	1.196	1.182	1.180
0.8	1.813	1.799	2.764	2.761	2.774

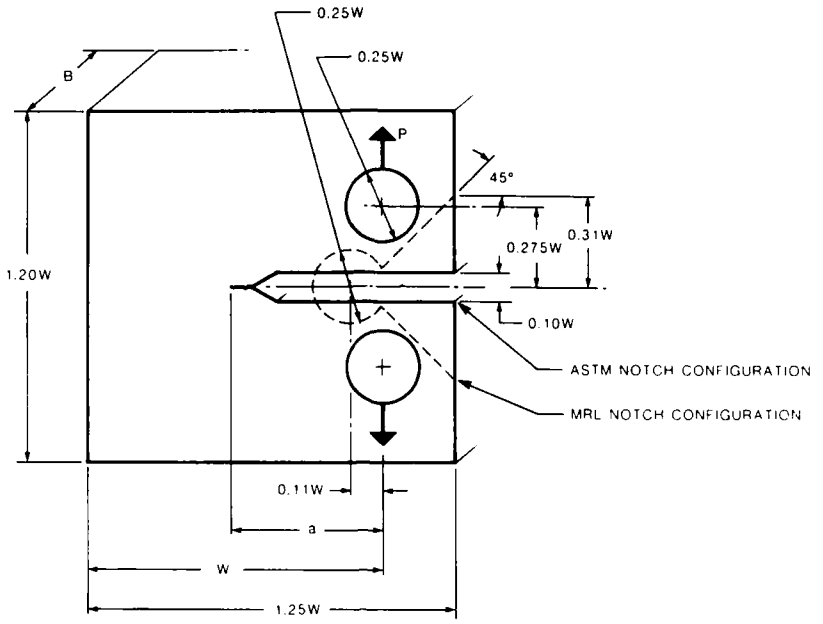

Figure 1 MRL and ASTM Compact Specimens

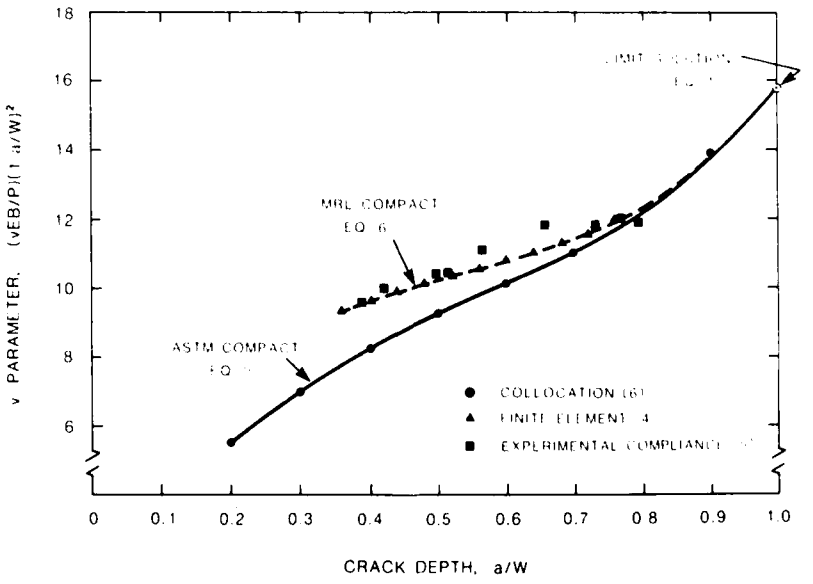

Figure 2 Load-Line-Displacement, v, for Compact Specimens

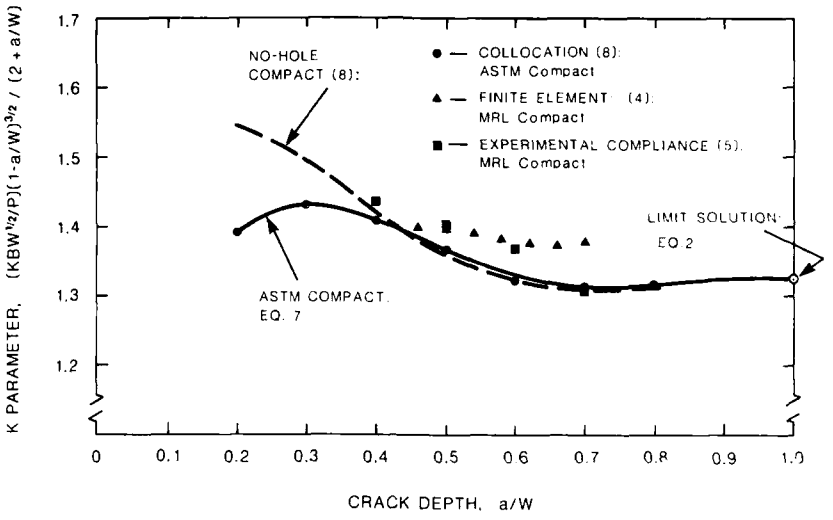

Figure 3 Stress Intensity Factor, K, for Compact Specimens

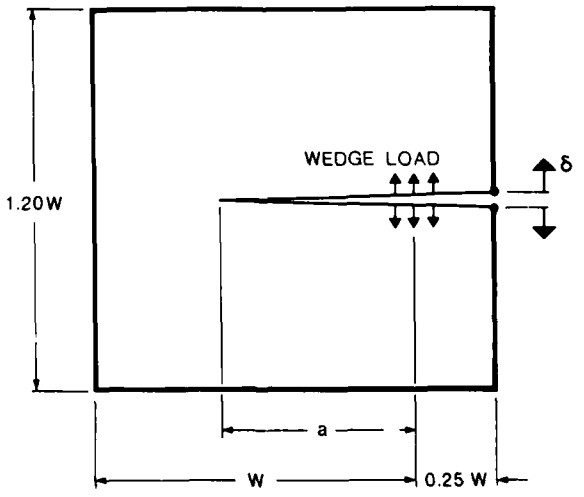

Figure 4 Wedge-Loaded Compact Specimen Geometry

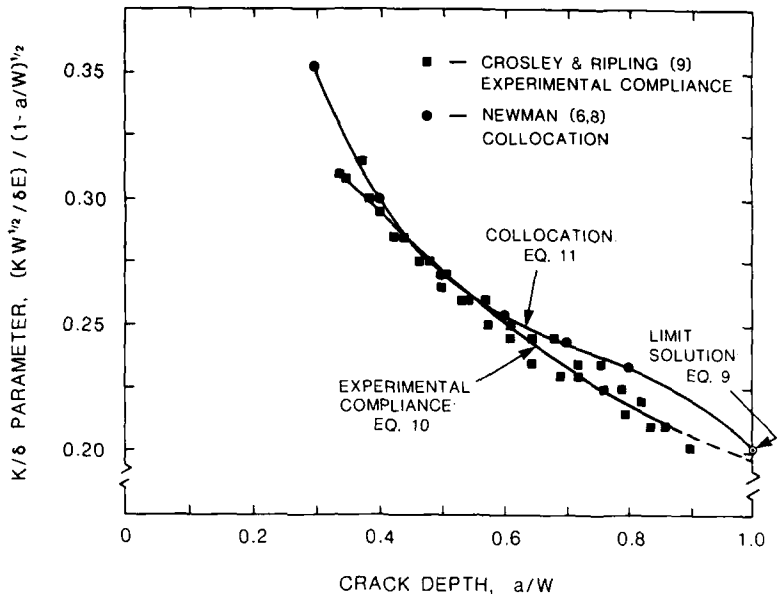

Figure 5 *Ratio of Stress Intensity Factor to Crack-Mouth-Displacement, K/δ, for Wedge-Loaded Compact Specimen*

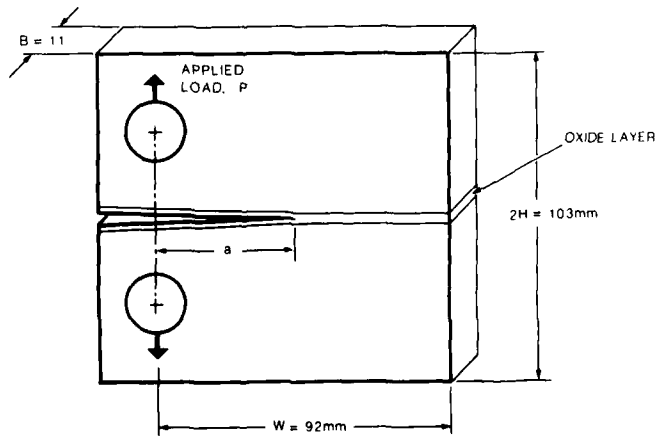

Figure 6 *Modified Compact Specimen for Brittle Coating Tests*

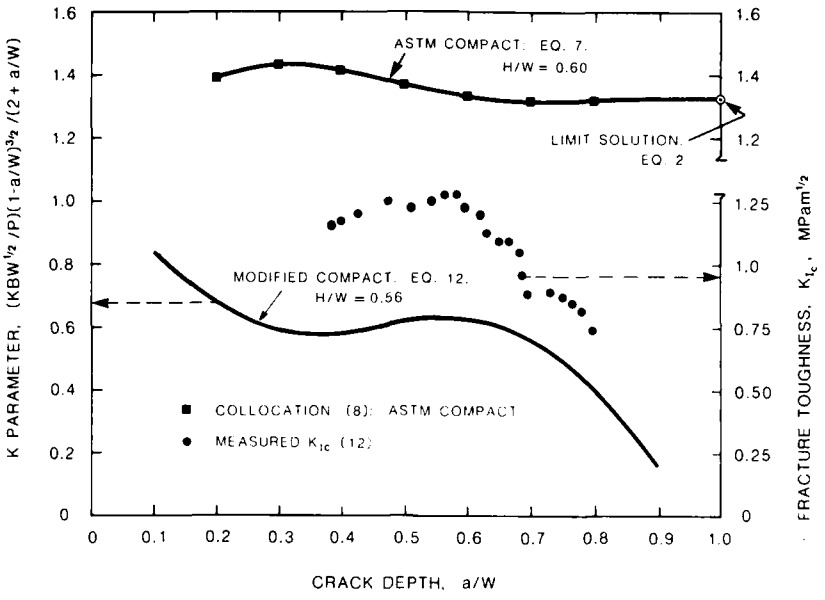

Figure 7 *Stress Intensity Factor, K, for Modified Compact Specimen Compared with K_{Ic} Measurements*

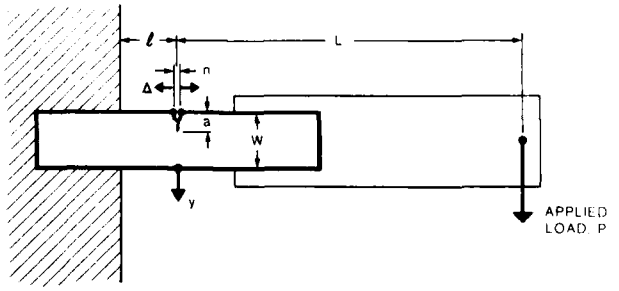

Figure 8 ***Cantilever-Loaded Bend Specimen Geometry***

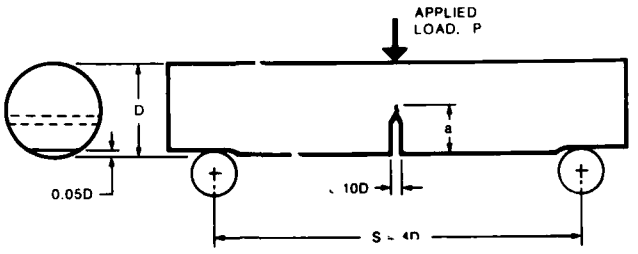

Figure 9 Round Bar Bend Specimen Geometry

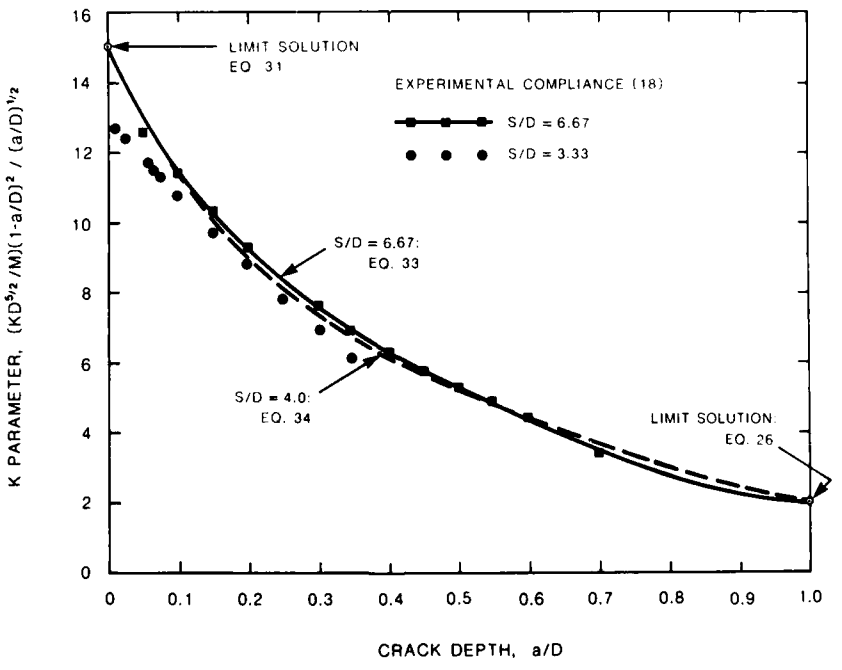

Figure 10 Stress Intensity Factor, K, for Round Bar Bend Specimen

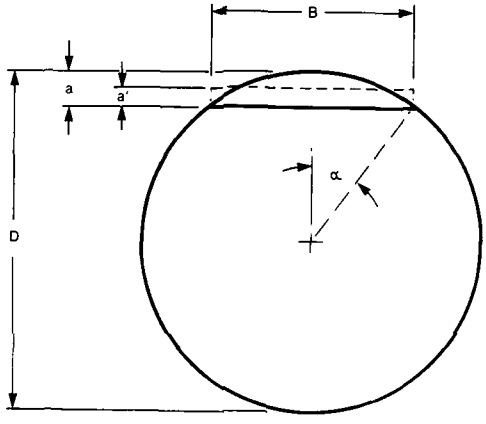

Figure 11 *Shallow Crack Geometry in a Round Bar Bend Specimen*

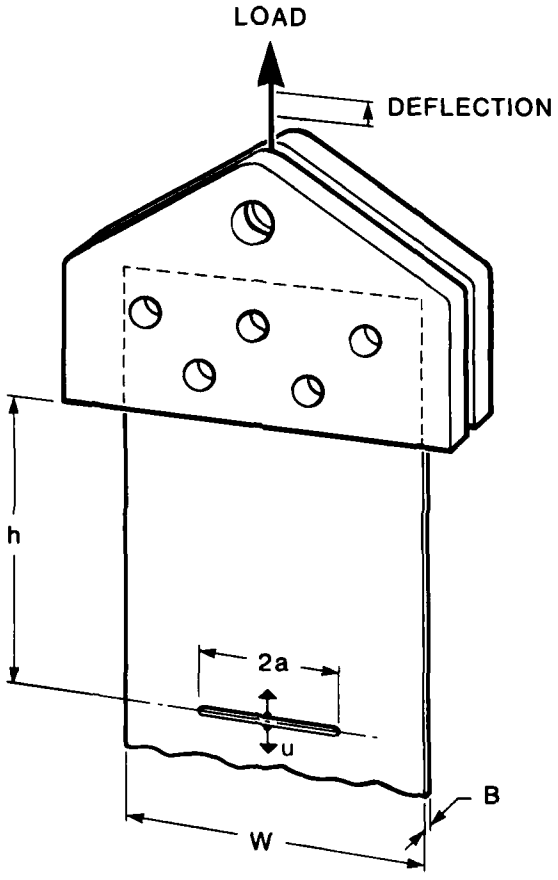

Figure 12 Tensile Panel for Composite Materials Tests

SECURITY CLASSIFICATION OF THIS PAGE **UNCLASSIFIED**

DOCUMENT CONTROL DATA SHEET

REPORT NO.	AR NO.	REPORT SECURITY CLASSIFICATION
MRL-TR-89-11	AR-005-698	Unclassified

TITLE

Analysis of some fracture mechanics test procedures for defence research applications

AUTHOR(S)
J.H. Underwood
I.A. Burch
M.Z. Shah Khan

CORPORATE AUTHOR
Materials Research Laboratory, DSTO
PO Box 50
Ascot Vale Victoria 3032

REPORT DATE	TASK NO.	SPONSOR
April 1989	NAV 87/140	NAV - Submarine Project Manager

FILE NO.	REFERENCES	PAGES
G6/4/8-3461	24	33

CLASSIFICATION/LIMITATION REVIEW DATE

CLASSIFICATION/RELEASE AUTHORITY
Chief, Materials Division MRL

SECONDARY DISTRIBUTION

Approved for Public Release

ANNOUNCEMENT

Announcement of this report is unlimited

KEYWORDS

Fracture (mechanics) Stress testing

SUBJECT GROUPS 0071G 0071L

ABSTRACT

Analysis has been presented of six fracture mechanics specimens and associated test procedures. Stress intensity factor results, and displacement results in some cases, have been compared for each specimen with numerical results and limit solutions from the literature. The specimens and test procedures analyzed are a compact specimen for general fracture testing, a crack arrest compact specimen, a modified compact specimen for brittle coating tests, a bend specimen for stress-corrosion cracking tests, a round bar bend specimen, and a tensile panel for composite material tests. Comparison with literature results was used to draw conclusions regarding accuracy of stress intensity factor and displacement relations for the specimens.